Fireside Corrosion Probes for Fossil Fuel Combustion

Bernard S. Covino, Jr., Sophie J. Bullard, Małgorzata Ziomek-Moroz, Gordon R. Holcomb
U.S. Department of Energy
Albany Research Center
Albany, OR
1450 Queen Ave, SW
Albany, OR 97321

David A. Eden
Intercorr International Inc.
14503 Bammel North Houston, Suite 300
Houston, TX 77014

ABSTRACT

Electrochemical corrosion rate probes have been constructed and tested along with mass loss coupons in environments consisting of $N_2/O_2/CO_2/SO_2$ plus water vapor. Temperatures ranged from 450° to 700°C. Results show that electrochemical corrosion rates for ash-covered mild steel are a function of time, temperature, and gaseous environment. Correlation between the electrochemical and mass loss corrosion rates was poor.

Keywords: corrosion, coal combustion, gaseous, electrochemical noise, harmonic distortion, linear polarization resistance, high temperature.

INTRODUCTION

Increasing the efficiency of the Rankine cycle in coal combustors can be accomplished by increasing heat exchanger steam temperatures and pressures as are done in supercritical and ultra supercritical units. The benefits of increasing energy conversion efficiencies are a reduced use of fossil fuels (coal, oil, and gas) and a reduced generation of greenhouse gases. In order to achieve both of these benefits, it will be necessary to overcome technological challenges related to materials of construction. New materials or material/coating combinations with adequate strength, creep, fatigue, and corrosion resistance will need to be developed. Additional issues are present when alternate fuels are used. While heat exchanger tubes in a coal-fired plants using clean high quality fuel may last 20 to 30 years, tubes in coal-fired plants using lower quality fuel, in Waste-to-Energy (WTE) plants[1], and in some coal gasification plants last only 3 to 5 years. Problems occur when equipment designed for either oxidizing or reducing conditions is exposed to alternating oxidizing and reducing conditions. The use of low NO_x burners is becoming more commonplace and can produce reducing environments. Complicating the development of corrosion-resistant materials for fireside applications is the influence of ash deposits and thermal gradients on the corrosion mechanism. Ash deposits and thermal gradients have a synergism that greatly increases the corrosive attack on equipment such as waterwalls, reheaters, and superheaters. One method of

addressing corrosion of these heat exchange surfaces is the use of corrosion sensors to monitor when process changes cause corrosive conditions. In such a case, corrosion rate could be a process control variable that directs the operation of a coal or waste combustion or coal gasification system. Alternatively, corrosion sensors could be used to monitor total metal damage which can be used as a tool to schedule planned maintenance outages.

There have been a number of research efforts aimed at developing high temperature corrosion probes for various industries. The majority of the research has been based on the use of electrochemical noise (EN)[2-7] techniques. Others have considered the use of electrochemical impedance spectroscopy (EIS)[4-6] and linear polarization resistance (LPR)[7], zero resistance ammetry (ZRA)[5], and electrical resistance (ER)[5]. There has been, however, only a limited effort reported to quantify[3] the operation of corrosion rate probes. Before these probes can be accepted routinely in the power generation industries, it will be necessary to determine if they accurately measure corrosion and the changes in corrosion that are occurring in a variety of environments, if the sensor materials have an optimum composition for the intended exposure, and if the sensitivity or accuracy of the sensor changes with length of time of exposure to fireside environments. Once this is established, electrochemical corrosion rate sensors can be used extensively and will allow corrosion rate to become a process variable for power plant operators.

This paper represents an update of a continuing research project aimed at developing high temperature electrochemical corrosion rate probes for use in fossil fuel ash-deposition environments. Previous research[8-10] has addressed issues of response, zero baseline, and quantitative nature of the corrosion probes. Research to be presented here will provide an update on the use of high temperature electrochemical corrosion rate probes.

EXPERIMENTAL DETAILS

Single three-sensor isothermal electrochemical corrosion rate (ECR) probes, as shown schematically in Figure 1, were designed and constructed for laboratory experiments using either mild carbon steel (CS), 304L stainless steel (SS), or 316L SS sensors (sensors are the same as electrodes used in a typical electrochemical cell). The two outer sensors in Figure 1 are the working and counter electrodes and the inner sensor is the reference electrode. Sensors were embedded within a plastic removable form using Ceramcast 586, a zirconia/magnesia potting compound. Ceramic pieces were embedded to provide a constant reference point for profilometry measurements. After curing, the probes were covered with ash using a slurry of ash with methanol and then exposed along with mass loss coupons made from the same material.

Two different types of ash were used in this research. The first was an ash from the Lee #1 Municipal Incinerator supplied by Covanta Energy, Inc. The second was a coal ash described as AEP TIDD Ash derived from Illinois #8 coal, and supplied by EERC, the University of North Dakota Energy and Environmental Research Center. Table 1 compares the composition of the two types of ash. Waste ash was used for the majority of the experiments discussed in this report. This ash shows high concentrations of corrosion-causing elements such as S, Cl, Pb, and K, all of which are able to form low melting point compounds and eutectic mixtures. The gas mixture consisted of 68 vol% N_2, 15 vol% H_2O, 9 vol% O_2, and 8 vol% CO_2. Water vapor was sometimes added to the gas stream. Temperatures ranged from 450 to 800°C and typical test periods were 100 to 500 hours. Coal ash was used for one experiment that ran for about 150 h. This ash notably lacks most of the corrosion-causing elements that are present in the waste ash. The gas mixture used consisted of 69 vol% N_2, 15 vol% CO_2, 10 vol% H_2O, 5 vol% O_2, and 1 vol% SO_2.

Isothermal probes are exposed nominally to the same temperature as the environment. These can be made as single or multi-probes. Multi-probes allow for increased amount of data for each experiment, where different alloys or different ashes can be exposed simultaneously in the same experiment. Air cooled probes contain a cooling chamber that allows the use of liquids or gases to adjust the temperature of the metallic sensors to a temperature of interest. Probes built and used to date were built for use in laboratory tube furnaces. Figure 2 shows a schematic of a typical air-cooled probe. This is intended as a prototype for field probes and also for future research to be conducted on the effect of thermal gradients on corrosion. Probes intended for use in field tests will incorporate features of air-cooled laboratory probes but also will need to be more rugged to survive the actual industrial environment.

The hardware used to measure the majority of the corrosion rates from the ECR probes was the SmartCET® Real-Time Corrosion Monitoring System[A]. This system used three separate electrochemical techniques: linear polarization resistance (hereafter referred to as LPR-1), electrochemical noise (EN), and harmonic distortion analysis (HDA). All three techniques measure a corrosion rate; EN also measures a localized (pitting) corrosion factor that varies from 0 to 1; and HDA measures the Tafel (βa, βc) constants used to calculate the Stern-Geary (B) constant. Corrosion rates and other variables are reported every 7 minutes and stored to computer using FieldCET® software[A]. Most of the corrosion rates in this report were taken from the LPR-1 measurements modified using the measured B values from each experiment. The default ECR probe corrosion rates were determined by integrating the LPR-1 corrosion rates to calculate the mass loss, which was then converted to a penetration rate with units of millimeters per year (mm/y).

Alternative electrochemical measurements were made using a PAR 273A potentiostat/galvanostat (hereafter referred to as Lab Potentiostat). Potentiodynamic polarization tests were conducted at 0.167 mV/s from -0.2 V vs open circuit potential (OCP) to +0.5 V vs the reference electrode. The middle of the three carbon steel or stainless steel sensors was used as the reference electrode. When pitting corrosion was suspected, the potential was reversed at +0.5 V vs OCP and scanned to -0.2V vs OCP. LPR measurements (hereafter referred to as LPR-2) were made at 0.167 V/s from -15 mV to +15 mV vs OCP. All electrochemical measurements were controlled by a computer operated with Corrware software.

All experiments were conducted in a 3-zone tube furnace containing a 2 in diameter alumina tube. Each zone was controlled with a separate temperature controller. Set temperatures for each zone were determined for each test temperature using an external calibration thermocouple and taking measurements at 1 cm intervals. For example, settings of 490, 510, and 400°C for zones 1, 2, and 3, respectively, gave an internal temperature of 500°C with a flat profile over 12 in (30.5 cm) of the 24 in (61 cm) heated zone. An alumina D-tube was inserted in the furnace tube to allow a platform for mass loss coupons. Measurement and control thermocouples were inserted in a 316 SS sheath that was then inserted in the D-tube.

Gas flows and thus gas mixture compositions were controlled using digital mass flow controllers that are controlled using Labview programs. Water vapor is added through an air-powered metering pump that pumps a specific quantity of water into a heated chamber and the water vapor is picked up by the test gas mixture.

RESULTS AND DISCUSSION

The results of this investigation are presented in terms of the following: (1) the operational nature of ECR probes which includes the issues of sensitivity to environmental changes and a quantitative or 1-to-1 correspondence between measured and actual corrosion rates; (2) the effect of different ashes on the response of ECR probes; and (3) the electrochemistry of the corrosion processes on ash-covered ECR probes.

Operational Nature of ECR Probes

One of the key operational features of corrosion rate probes is that they should be responsive to changes in conditions. Figure 3 shows a 500 h exposure test for a waste ash-coated 304 SS ECR probe in a $N_2/O_2/CO_2$ gaseous environment. The probe was heated to temperature in 100 vol % N_2 and allowed to remain in N_2 for about 165 h. During this time the corrosion rate remained high at 4-5 mm/y, decreasing slightly. After 165 h, the gas composition was changed to 68 vol % N_2/9 vol % O_2/8 vol % CO_2which caused the corrosion rate to decrease to about 1 mm/y at 230 h. Here the gas was again switched to 100 vol % N2 which again caused the corrosion rate to increase to 4-5 mm/y. After peaking at 4.8 mm/y, the corrosion rate started decreasing. The addition of 8 vol % CO_2 at 250 h continued the decrease in corrosion rate but with a change in slope. The addition of 9 vol % O_2 at 295 h again continued the decrease in corrosion rate with yet another change in slope. This experiment

[A] InterCorr International, Houston, TX USA; recently acquired by Honeywell and operating as part of Honeywell Process Solutions

shows that both O_2 and CO_2 cause the corrosion rate of the ash-covered 304 SS to decrease as soon as those gases are present while corrosion rates in N_2 decrease only after a time delay.

Another feature of ECR probes is that corrosion rates should follow past experiences. For example, it is well known that higher alloys corrode less than lower alloys and that higher temperatures (except around 700°C when molten sulfates are present, for example) generally cause higher corrosion rates. The data in Table 2 show that the ECR probes do behave as expected. Corrosion rates increased with increasing temperatures for both alloys and 316 SS corroded less than carbon steel under equivalent conditions. In a similar manner, it is known that different types of ash are more corrosive than others. Research conducted here has shown that the waste ash presents a considerably more corrosive environment than the coal ash that is being used in this research. Data in Table 3 show that the ECR probe measured a higher corrosion rate in the waste ash than in the coal ash. Newly cleaned boiler tubes have been reported to have a layer of FeS deposited before ash starts accumulating. One experiment shown in Table 3 was designed to simulate this phenomenon. Measurements showed that the corrosion rate was much higher due to the FeS layer. Table 4 shows that higher corrosion rates were measured when more water vapor was added to the gaseous environment.

An important operational feature of electrochemical corrosion rate probes is that they produce measurements that are equivalent to the actual corrosion rate of a structure. This would mean that the measurements were quantitative. If this is not the case, then it is essential that the signal be proportional in a regular manner to the corrosion rate. This would make the measurements semi-quantitative and would require a calibration curve or calibration factor. Our approach to understanding the quantitative nature of ECR probes is to use mass loss coupons embedded in ash and exposed at the same time and to the same conditions as the ECR probe. Mass loss coupons removed from experiments were cleaned of all ash and corrosion deposits and weighed to determine weight loss due to corrosion. Corrosion penetration rates were then calculated using weight loss, exposed area, and exposure time. Electrochemical corrosion rates for the ECR probes were calculated either by: (1) converting corrosion rates to weight loss for each 7 min measurement period, summing the weight losses, and then converting to corrosion penetration rates as above, or (2) calculating an average corrosion rate over the exposure time period. Both techniques gave nearly identical answers.

Corrosion rate calculations from mass loss, LPR-1, and EN data were evaluated and the results are presented in Table 5. It shows a comparison of ratios of Real-Time Corrosion Monitoring LPR-1 and EN corrosion rates to corrosion rates determined in the same experiment from mass loss (ML) coupons. The Real-Time Corrosion Monitoring LPR-1 and EN corrosion rates are calculated based on using the best measured Stern-Geary constant (B) as shown in equation (1). The results in Table 5 show that the ratio of LPR corrosion rates to ML corrosion rates ranges from 0.05 to 9.6 and the ratio of LPR corrosion rates to EN corrosion rates ranges from 0.08 to 19.9. A ratio of 1 would indicate that there is a one-to-one relationship between either the LPR or EN corrosion rates and the ML corrosion rates, and therefore quantitative behavior. The data in Table 5 suggests that both the LPR and EN techniques produce corrosion rates that are semi-quantitative. A ratio of greater than one indicates that the electrochemical technique (LPR or EN) measures less of the corrosion reaction than actually occurs for the ML samples. A ratio of less than one indicates that the electrochemical technique measures not only the corrosion reaction but other electrochemical reactions as well. The data in Table 5 further indicate that the former case occurs for the waste ash covered alloys and the latter for the coal ash covered alloys. The difference between these two ashes (see Table 1) is the larger quantity of K, Pb, Na, and Cl in the waste ash. If these elements in the waste ash are able to form low melting point molten salts, those molten salts could cause chemical dissolution that would not be measured as an electrochemical reaction. It is not clear what other electrochemical reactions are occurring in coal ash. Research is underway to understand this semi-quantitative behavior and to determine calibration factors for the probes.

Effect of Ash Composition on ECR Probe Response

Figure 4 shows the typical response of a 304 SS ECR probe coated with waste ash. An expansion of the beginning of the experiment (not shown) indicates that a small amount of corrosion occurred when the ash/methanol slurry was applied to the probe before heat-up. Also evident was the fact that the corrosion rate increase lagged behind the temperature increase until approximately 400°C. Corrosion rate was typically unstable

for a period of time after the addition of the gaseous environment. After that point the corrosion rate decreased over a period of 50 to100 h.

Figure 5 shows the typical response of a 304 SS ECR probe coated with coal ash. An expansion of the beginning of the experiment would show a small amount of corrosion when the ash/methanol slurry was applied to the probe before heat-up. Also visible would be the fact that the corrosion rate increase lags behind the temperature increase until approximately 400°C. In coal ash, however, the corrosion rate is much lower at the beginning of the experiment than that shown in Figure 3. Another interesting phenomenon is that when the $N_2/CO_2/O_2/SO_2$ environment was added, the corrosion rate did not increase. The corrosion rate did finally start increasing 24 h later when water vapor was added to the environment. Corrosion rates did not decrease with time as shown in Figure 4 for the waste ash-covered 304 SS ECR probe.

The localized corrosion or pitting factor is an indication of the probability of pitting that is reported from the EN technique. The pitting factor (PF) ranges from 0 to 1 but is best divided into logarithmic decades of 0.001 to 0.01 (no probability of localized corrosion), 0.01 to 0.1 (slight probability of localized corrosion), and 0.1 to 1 (high probability of localized corrosion). In all of the experiments conducted on ECR probes covered with waste ash, there was never an indication of the possibility of localized corrosion. This is despite the fact that the waste ash contains high levels of chlorides (Table 1). Results were different for the coal-ash-covered ECR probe. Figure 5 shows the pitting factor to be in the highest range suggesting a high probability of pitting.

Electrochemical Behavior of Ash-Covered ECR Probes

Electrochemical measurements were conducted using a standard laboratory potentiostat to verify the accuracy of the Real-Time Corrosion Monitoring measurements, to show that other types of equipment can be used reliably to make similar measurements, and to attempt to understand the electrochemical nature of the corrosion reactions on the ash covered probes. These measurements were taken by interrupting and disconnecting the Real-Time Corrosion Monitoring system, allowing the Lab Potentiostat to be connected. The potentiodynamic polarization behavior of a waste ash-covered 304 SS ECR probe is shown in Figure 6. This curve is typical of an actively corroding metal and suggests that all or part of the corrosion reactions are electrochemical in nature. The linear part of the curve near the corrosion potential in Figure 6 was further analyzed to derive the potentiodynamic (PD) polarization resistance, Rp. Rp was then converted to a PD corrosion rate for comparison to the Real-Time Corrosion Monitoring LPR corrosion rate. Standard LPR-2 tests were also conducted (not shown) and the data converted to a corrosion rate. All of these measurements are compared in Table 6.

The measurements in Table 6 show a good agreement between the Lab Potentiostat (LPR-2) and the Real-Time Corrosion Monitoring LPR corrosion rates (LPR-1). The potentiodynamic (PD) corrosion rates are actually close to the Real-Time Corrosion Monitoring LPR corrosion rates, but not quite as good as the PAR LPR corrosion rates. This is to be expected because of the different parameters used to make the PAR LPR and PAR PD measurements.

Electrochemical tests on a coal-ash-covered 304 SS ECR probe, shown in Figure 7, show a more complicated potentiodynamic polarization behavior. Part of the reason for this is that the potential was reversed at 0.5 V vs OCP in order to determine if pitting was occurring. Another reason is that the more resistive ash caused the electrochemical behavior to be noisy, requiring smoothing to produce the curve in Figure 7. The polarization curve in Figure 7 suggests active-passive behavior, pitting breakdown (a pitting potential, E_p), and a repassivation potential (E_{rp}).

CONCLUSIONS

- ECR probe corrosion rates are sensitive to changes in temperature and environment gas composition.
- Both the LPR and EN techniques appear to produce corrosion rates that are semi-quantitative in nature.
- Ash from a waste incineration process is more corrosive than coal ash based on the combustion of Illinois No. 8 coal.

- Electrochemical measurements confirm that at least some of the corrosion reaction is electrochemical in nature.
- There is a good correlation between corrosion rates measured using Real-Time Corrosion Monitoring electrochemical technology to those measured using a standard potentiostat.

REFERENCES

1. H. Thielsch and F. M. Cone, "Remedies for WTE's Most Vexing O&M Problem: Tube Failure," Solid Waste Technologies, January-February, pp 32-39, 1994.
2. T.M. Linjeville, K.A. Davis, G.C. Green, W.M. Cox, R.N. Carr, N.S. Harding, and D. Overacker, "On-Line Technique for Corrosion Characterization in Utility Boilers, Proceedings of Power Production in the 21st Century: Impacts of Fuel Quality and Operations," United Engineering Foundation, Snowbird, UT, October 28-November 2, 2001.
3. T.M. Linjeville, J. Valentine, K.A. Davis, N.S. Harding, and W.M. Cox, "Prediction and Real-time Monitoring techniques for Corrosion Characterization in Furnaces," Materials at High Temperatures, Vol. 20, No. 2, pp. 175-184, 2003.
4. D.M. Farrell, W.Y. Mok, and L.W. Pinder, "On-line Monitoring of Furnace-Wall Corrosion in a 125 MW Power Generation Boiler," Materials Science and Engineering, Vol. A121, pp. 651-659, 1989.
5. D. M. Farrell, "On-line Monitoring of Fireside Corrosion in Power Plant," 12th International Corrosion Congress, Vol. 12, pp. 4131-4140, 1993.
6. G. Gao, F.H. Stott, J.L. Dawson, and D.M. Farrell, "Electrochemical Monitoring of High-Temperature Molten Salt Corrosion," Oxidation of Metals, Vol. 33, Nos. 1/2, pp. 79-94, 1990.
7. G.J. Bignold and G.P. Quirk, "Electrochemical Noise Measurements in a 500 MW Steam Turbine to Maximize Lifetime Under Changing Operational Demands," Paper no, 02333, CORROSION/2002, NACE International, Houston, TX, 20 pp, 2002.
8. B. S. Covino, Jr., S. J. Bullard, S. D. Cramer, G. R. Holcomb, M. Ziomek-Moroz, D. A. Eden, R. D. Kane, and D. C. Eden, "High Temperature Electrochemical Noise Corrosion Sensors For Fossil Fuel Combustion," Paper No. 04528, Corrosion/2004 (New Orleans, LA, March 28-April 1, 2004), NACE International, Houston TX, 2004, 9 pp.
9. B. S. Covino, Jr., S. J. Bullard, S. D. Cramer, G. R. Holcomb, M. Ziomek-Moroz, D. A. Eden, and M. S. Cayard, "Electrochemical Corrosion Rate Probes for High Temperature Energy Applications," Proceedings of the Fourth International Conference on Advances in Materials Technology in Fossil Power Plants, Hilton Head Island, South Carolina, October 25-28, 2004.
10. B. S. Covino, Jr., S. J. Bullard, S. D. Cramer, G. R. Holcomb, M. Ziomek-Moroz, R. D. Kane, and D. C. Eden, "Monitoring Power Plant Fireside Corrosion Using Corrosion Probes," Proceedings of the 30th International Technical Conference on Coal Utilization & Fuel Systems, Coal Technology Association, Clearwater, FL, April 17-21, 2005.

Table 1
Composition (wt %) of major corrosion-causing elements in 2 combustion ashes used in ECR probe research.

Ash	Al	K	Pb	Na	Cl	Fe	S
Waste	3.6	3.7	2.7	3.5	6.7	5	6.5
Coal	4.0	trace	0	trace	0	4.5	6

Table 2
Effect of alloy and temperature on Real-Time Corrosion Monitoring LPR-1 corrosion rate measurements

Alloy	Temp, °C	ECR, mm/y
Carbon Steel	450	0.89
Carbon Steel	500	2.74
316 SS	500	0.28
316 SS	600	3.73

Table 3
Effect of ash type on Real-Time Corrosion Monitoring LPR-1 corrosion rate measurements

Alloy	Ash	ECR, mm/y
316 SS	Waste	0.28
316 SS	Coal	0.005
316 SS	Coal + FeS	1.44

Table 4
Effect of water content on Real-Time Corrosion Monitoring LPR-1 corrosion rate measurements

Alloy	% H_2O	ECR, mm/y
304 SS	0	0.563
304 SS	14	1.1

Table 5
Real-Time Corrosion Monitoring LPR-1 and EN Corrosion rate ratios with ML corrosion rates for select experiments.

Alloy	Ash	ML/LPR	ML/EN
CS	Waste	9.6	19.9
304 SS	Waste	4.2	9.7
304 SS	Waste	6.5	8.5
316 SS	Waste	1.4	3.2
316 SS	Waste	12.9	7.6
304 SS	Coal	0.35	0.31
316 SS	Coal + FeS	0.05	0.08
ML = mass loss corrosion rates, LPR-1 = LPR probe corrosion rates, and EN = electrochemical noise probe corrosion rates			

Table 6
Comparison of Real-Time Corrosion Monitoring LPR-1, Lab Potentiostat LPR-2, and Lab Potentiostat PD (potentiodynamic) corrosion rates, mm/y

LPR-1	LPR-2	PD
0.0028	0.0008	NA
1.83	1.63	NA
1.79	1.65	1.52
0.66	0.60	0.45
0.44	0.41	0.30
1.44	1.28	0.91
0.15	0.14	0.14

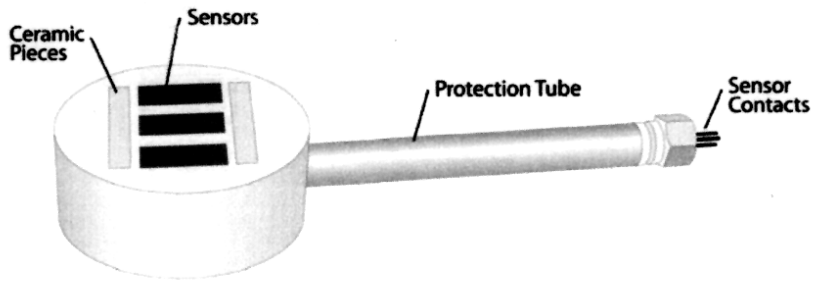

Figure 1: Schematic representation of a typical ECR probe

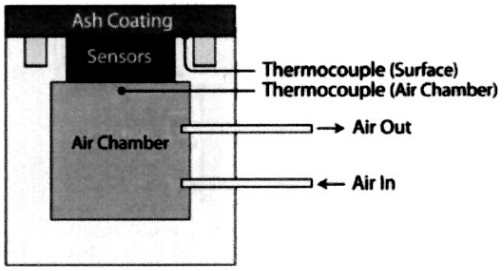

Figure 2 – Schematic cross-section of a typical air-cooled ECR probe showing sensors, air chamber, air tubes, and thermocouples.

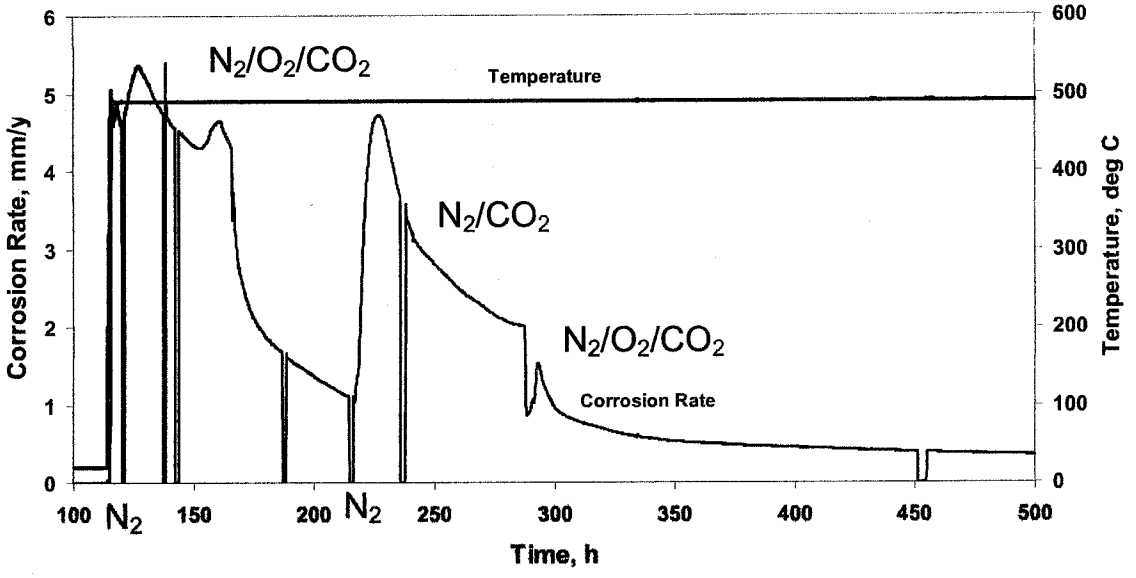

Figure 3 – Effect of changing gas composition on the Real-Time Corrosion Monitoring-measured corrosion rate of a 304 SS ECR probe. Note that corrosion rate excursions to 0 mm/y occurred when the Real-Time Corrosion Monitoring system was disconnected to allow electrochemical measurements using a laboratory potentiostat.

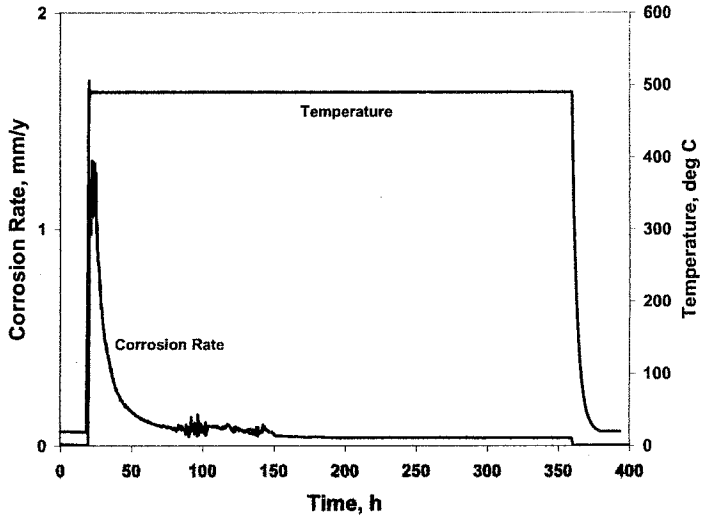

Figure 4 – Real-Time Corrosion Monitoring LPR Corrosion rate response of waste ash-covered 304SS ECR Probe at 500°C.

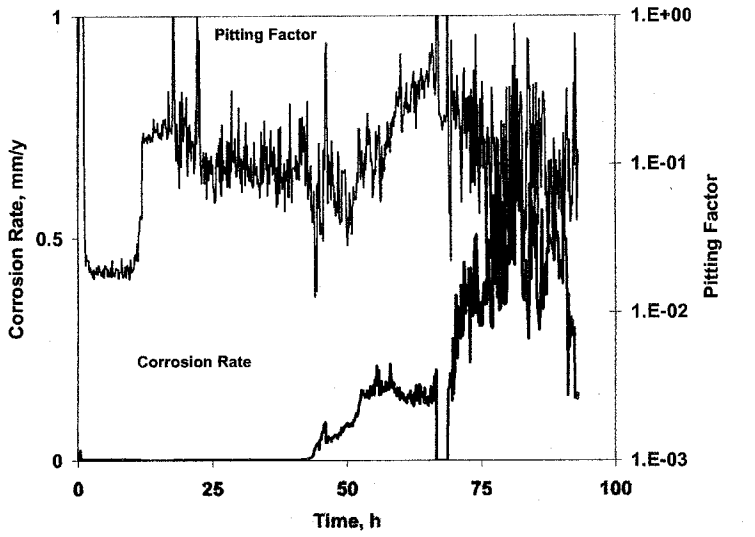

Figure 5 – Real-Time Corrosion Monitoring LPR Corrosion rate and pitting factor as a function of time for a coal-ash-covered 304 SS ECR probe at 500°C.

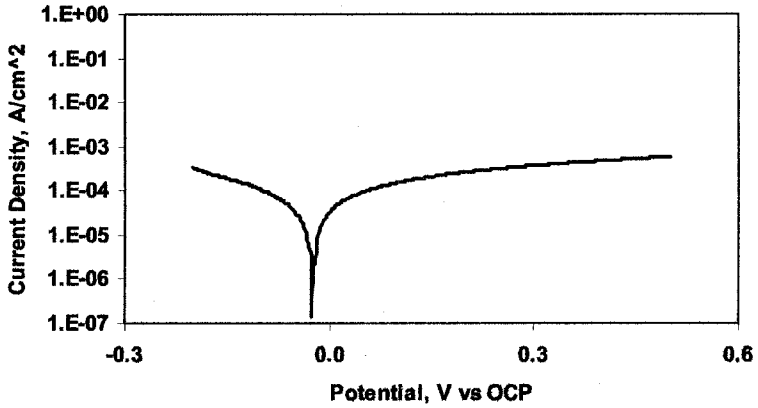

Figure 6 – Potentiodynamic polarization curve of a waste ash-covered 304 SS ECR probe at 500°C. Potentials were measured versus an unpolarized 304 SS sensor

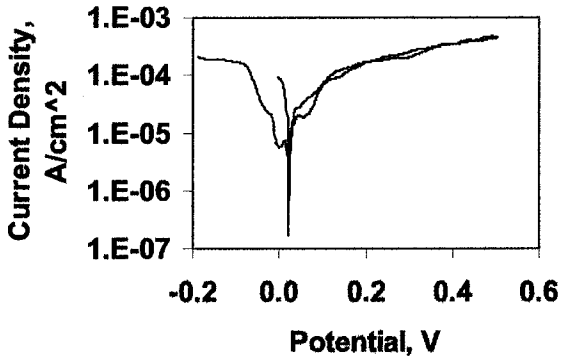

Figure 7 –Potentiodynamic polarization behavior of a coal-ash-covered 304 SS ECR probe at 500°C. Potentials were measured versus an unpolarized 304 SS sensor.